The N-Localizer and Volume Imaging

Russell A. Brown [1]

1. Principal Engineer, A9.com

✉ **Corresponding author:** Russell A. Brown, russ.brown@yahoo.com
Disclosures can be found in Additional Information at the end of the article

Abstract

The mathematics that were originally developed for the N-localizer apply to three N-localizers that produce three sets of fiducials in a planar, tomographic image. Recently, these mathematics have been extended to apply to three or more sets of fiducials in a planar, tomographic image. This paper discusses a further extension of the mathematics of the N-localizer that applies to volume images that are produced by magnetic resonance (MR) imaging. This extension of the mathematics applies to four or more N-localizers that are visualized in more than one planar section of the volume image. In addition, this extension provides a statistical measure of the quality of the volume image data that may be influenced by factors such as nonlinear distortion of MR images.

Introduction

Recent review articles discuss the origin and mathematics of the N-localizer [1-5]. The mathematics are summarized briefly in the remainder of this Introduction in preparation for the presentation of new developments in the Materials & Methods section of this article.

The N-localizer comprises a diagonal rod that extends from the top of one vertical rod to the bottom of another vertical rod (Figure 1). Assuming for the sake of simplicity that the two vertical rods are perpendicular to the tomographic section, the cross section of each vertical rod creates a fiducial circle and the cross section of the diagonal rod creates a fiducial ellipse in the tomographic image. The ellipse moves away from one circle and towards the other circle as the position of the tomographic section moves downward with respect to the N-localizer. The relative spacing between these three fiducials permits precise localization of the tomographic section relative to the N-localizer. The distance d_{AB} between the centers of circle A and ellipse B and the distance d_{AC} between the centers of circles A and C are used to calculate the ratio $f = d_{AB}/d_{AC}$. This ratio represents the fraction of diagonal rod B that extends from the top of vertical rod A to the point of intersection of rod B with the tomographic section. These geometric relationships are valid even if the vertical rods are not perpendicular to the tomographic section [6]; in this case, the cross sections of the vertical rods may be somewhat elliptical, depending on the degree of nonperpendicularity.
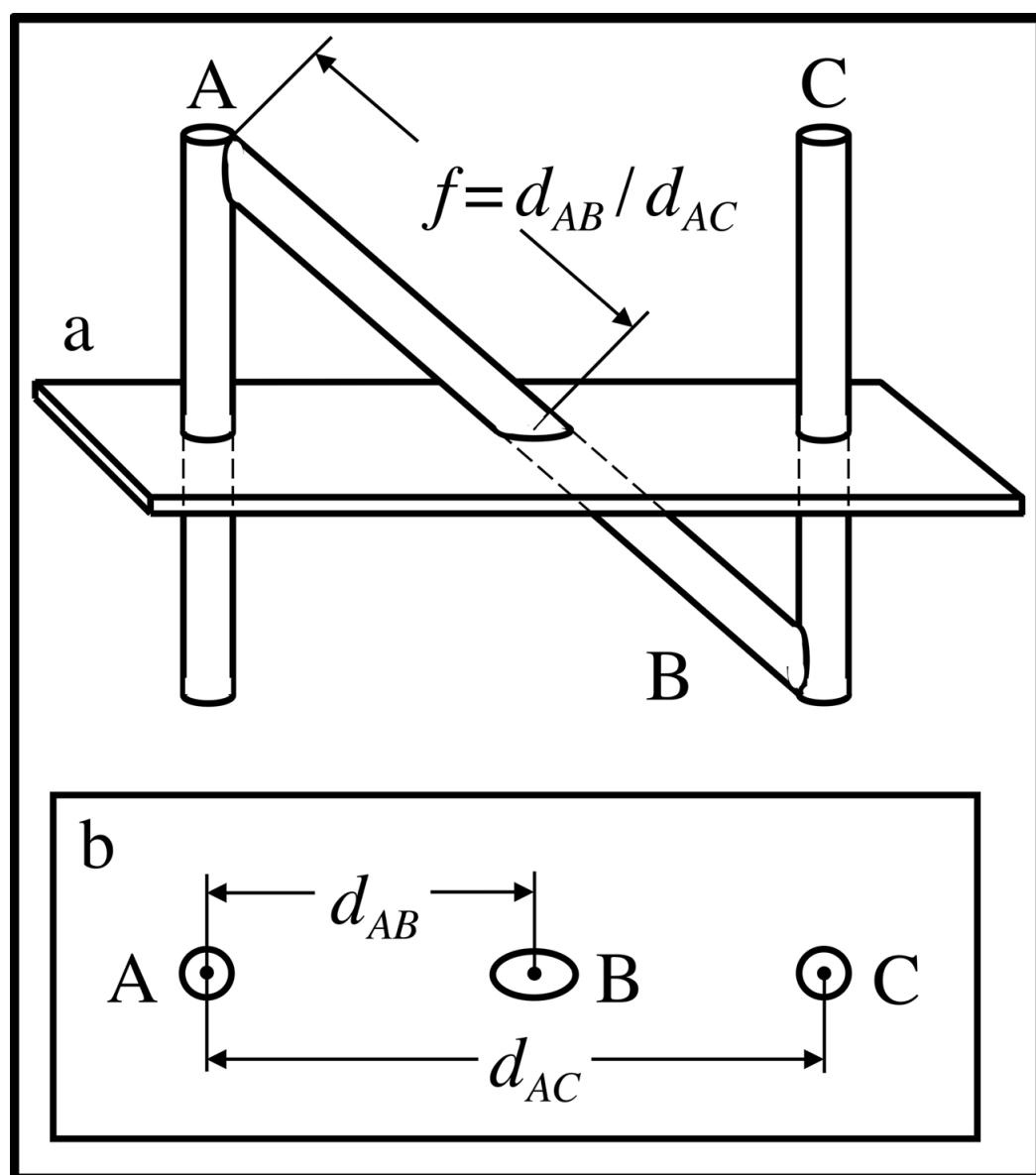
FIGURE 1: Intersection of the tomographic section with the N-localizer

$(\mathbf{a})$ Side view of the N-localizer. The tomographic section intersects rods A, B and C. $(\mathbf{b})$ Tomographic image. The intersection of the tomographic section with rods A, B and C creates fiducial circles A and C and fiducial ellipse B in the tomographic image. The distance d_{AB} between the centers of circle A and ellipse B and the distance d_{AC} between the centers of circles A and C are used to calculate the ratio $f = d_{AB}/d_{AC}$. This ratio represents the fraction of diagonal rod B that extends from the top of rod A to the point of intersection of rod B with the tomographic section.

The fraction f is used to calculate the (x, y, z) coordinates of the point of intersection P'_B between rod B and the tomographic section (Figure 2). In this figure, points P'_A and P'_C represent the beginning and end, respectively, of the vector that extends from the top of rod A to the bottom of rod C. This vector coincides with the long axis of rod B. The (x_A, y_A, z_A) coordinates of the beginning point P'_A and the (x_C, y_C, z_C) coordinates of the end point P'_C are known from the physical dimensions of the N-localizer. Hence, linear interpolation may be used to blend points P'_A and P'_C to obtain the (x_B, y_B, z_B) coordinates of the
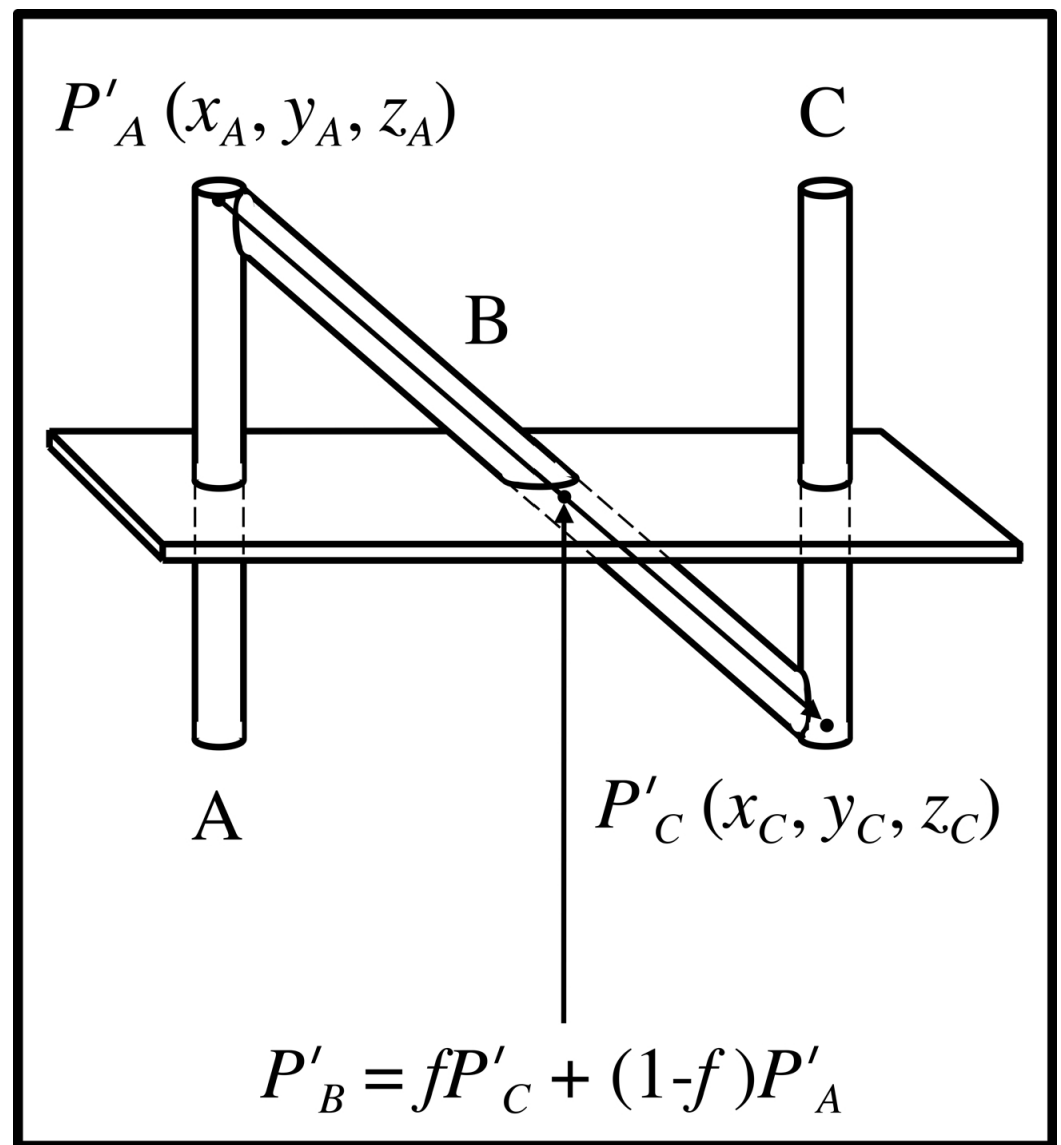
point of intersection P'_B between the long axis of rod B and the tomographic section

$$P'_B = P'_A + f\left(P'_C - P'_A\right) = fP'_C + (1-f)\,P'_A \qquad (1)$$

The vector form of Equation 1 shows explicitly the (x, y, z) coordinates of points P'_A, P'_B, and P'_C

$$[x_B\ y_B\ z_B] = f\,[x_C\ y_C\ z_C] + (1-f)\,[x_A\ y_A\ z_A] \qquad (2)$$

Equation 1 or 2 may be used to calculate the (x_B, y_B, z_B) coordinates of the point of intersection P'_B between the long axis of rod B and the tomographic section. The point P'_B, which lies on the long axis of rod B in the three-dimensional coordinate system of the N-localizer, corresponds to the analogous point P_B, which lies at the center of ellipse B in the two-dimensional coordinate system of the tomographic image. Hence, there is a one-to-one correspondence between a point from the N-localizer and a point from the tomographic image.

FIGURE 2: Calculation of the point of intersection between the rod B and the tomographic section

The long axis of rod B is represented by a vector that extends from point P'_A at the top of rod A to point P'_C at the bottom of rod C. The (x_A, y_A, z_A) coordinates of point P'_A and the (x_C, y_C, z_C) coordinates of point P'_C are known from the physical dimensions of the N-localizer. Hence, the ratio $f = d_{AB}/d_{AC}$ may be used to blend the (x_A, y_A, z_A) and (x_C, y_C, z_C) coordinates of points P'_A and P'_C via linear interpolation as indicated by Equations 1 and 2. This interpolation calculates the (x_B, y_B, z_B) coordinates of the point of intersection P'_B between the long axis of rod B and the tomographic section.

The attachment of three N-localizers to a stereotactic frame (Figure 3) permits calculation of the $(x_{B_1}, y_{B_1}, z_{B_1})$, $(x_{B_2}, y_{B_2}, z_{B_2})$, and $(x_{B_3}, y_{B_3}, z_{B_3})$ coordinates for the three respective points P'_{B_1}, P'_{B_2}, and P'_{B_3} in the three-dimensional coordinate system of the stereotactic frame. These three points correspond respectively to the three analogous points P_{B_1}, P_{B_2}, and P_{B_3} in the two-dimensional coordinate system of the tomographic image. In the following discussion, the symbols P'_1, P'_2, and P'_3 will be used as a shorthand notation for P'_{B_1}, P'_{B_2}, and P'_{B_3}. The symbols P_1, P_2, and P_3 will be used as a shorthand notation for P_{B_1}, P_{B_2}, and P_{B_3}.
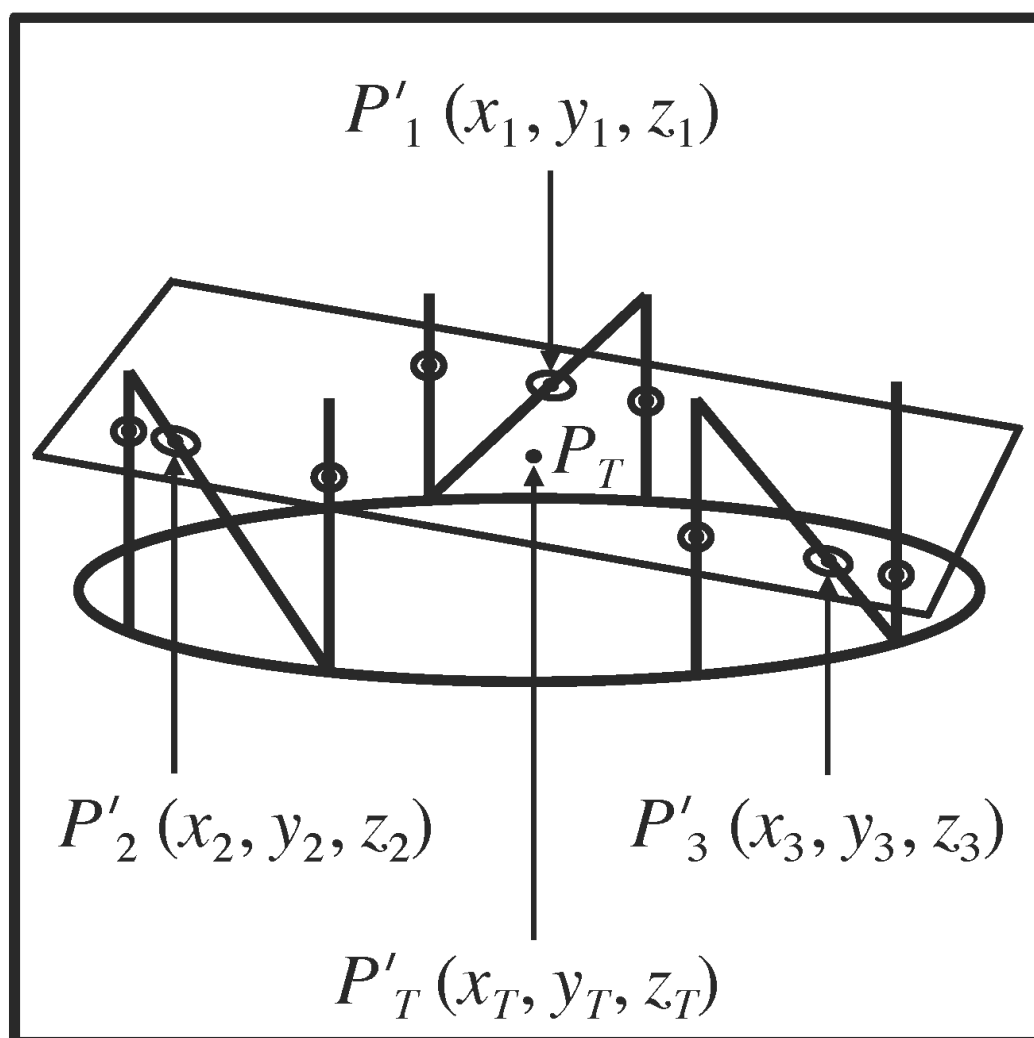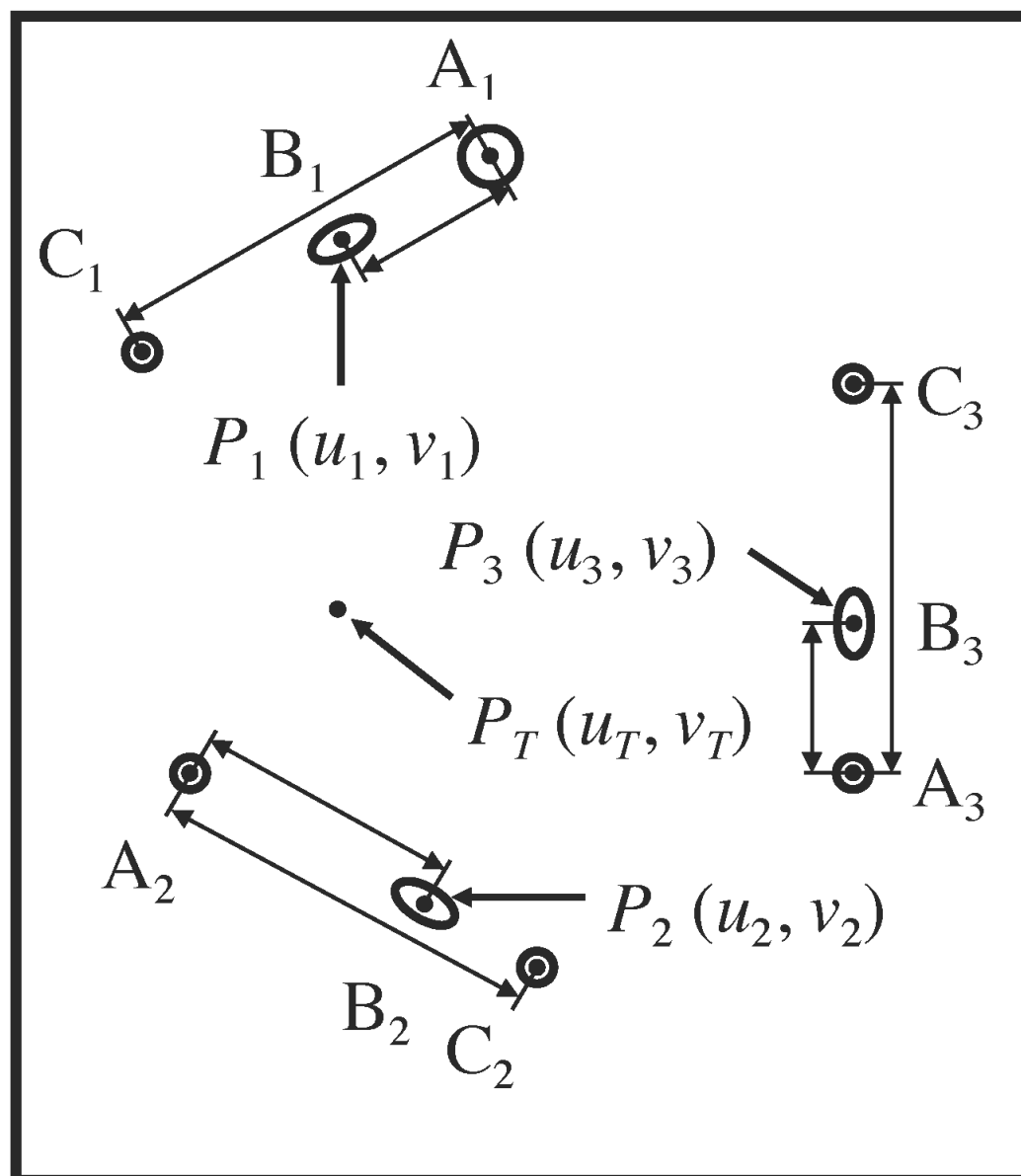

FIGURE 3: Representation of the tomographic section in the three-dimensional coordinate system of the stereotactic frame

The quadrilateral represents the tomographic section. The large oval depicts the base of the

stereotactic frame. The vertical and diagonal lines that are attached to the large oval represent the nine rods. The centers of the six fiducial circles and the three fiducial ellipses that are created in the tomographic image by these nine rods are shown as points that lie in the tomographic section. The tomographic section intersects the long axes of the three diagonal rods at points P'_1, P'_2 and P'_3 that coincide with the respective centers P_1, P_2 and P_3 of the three ellipses (Figure 4). The (x_1, y_1, z_1), (x_2, y_2, z_2) and (x_3, y_3, z_3) coordinates of the respective points of intersection P'_1, P'_2 and P'_3 are calculated in the three-dimensional coordinate system of the stereotactic frame using Equations 1 and 2. Because these three points determine the spatial orientation of a plane in three-dimensional space, the spatial orientation of the tomographic section is determined relative to the stereotactic frame. The target point P'_T lies in the tomographic section. The (x_T, y_T, z_T) coordinates of this target point are calculated in the three-dimensional coordinate system of the stereotactic frame using Equation 5.

The three points, P'_1, P'_2, and P'_3, lie on the long axes of the three respective diagonal rods, B_1, B_2, and B_3, and have respective (x, y, z) coordinates (x_1, y_1, z_1), (x_2, y_2, z_2), and (x_3, y_3, z_3) in the three-dimensional coordinate system of the stereotactic frame (Figure 3). The analogous three points, P_1, P_2, and P_3, lie at the centers of the three respective ellipses, B_1, B_2, and B_3, and have (u, v) coordinates (u_1, v_1), (u_2, v_2), and (u_3, v_3) in the two-dimensional coordinate system of the tomographic image (Figure 4).

FIGURE 4: Representation of the two-dimensional coordinate system of the tomographic image

The cross sections of three N-localizers create three sets of fiducials $\{A_1, B_1, C_1\}$, $\{A_2, B_2, C_2\}$ and $\{A_3, B_3, C_3\}$ in a tomographic image. Each set contains two circles and one ellipse that are collinear. For each set, the short double-ended arrows indicate the distance d_{AB} between the centers of circle A and ellipse B and the long double-ended arrows indicate the distance d_{AC} between the centers of circles A and C. The centers P_1 , P_2 and P_3 of the three ellipses coincide with the respective points of intersection P_1' , P_2' and P_3' of the long axes of the three diagonal rods with the tomographic section (Figure 3). The (u_1, v_1) , (u_2, v_2) and (u_3, v_3) coordinates of the centers P_1 , P_2 and P_3 correspond respectively to the (x_1, y_1, z_1) , (x_2, y_2, z_2) and (x_3, y_3, z_3) coordinates of the points of intersection P_1' , P_2' and P_3' . A target point P_T has (u_T, v_T) coordinates in the two-dimensional coordinate system of the tomographic image. The (x_T, y_T, z_T) coordinates of the analogous target point P_T' are calculated in the three-dimensional coordinate system of the stereotactic frame using Equation 5.

Because three points determine the orientation of a plane in three-dimensional space, the

three coordinates, (x_1, y_1, z_1), (x_2, y_2, z_2), and (x_3, y_3, z_3), together with the three coordinates, (u_1, v_1), (u_2, v_2), and (u_3, v_3), determine the spatial orientation of the tomographic section relative to the stereotactic frame. This spatial orientation is specified using the matrix equation

$$\begin{bmatrix} x_1 & y_1 & z_1 \\ x_2 & y_2 & z_2 \\ x_3 & y_3 & z_3 \end{bmatrix} = \begin{bmatrix} u_1 & v_1 & 1 \\ u_2 & v_2 & 1 \\ u_3 & v_3 & 1 \end{bmatrix} \begin{bmatrix} m_{11} & m_{12} & m_{13} \\ m_{21} & m_{22} & m_{23} \\ m_{31} & m_{32} & m_{33} \end{bmatrix} \qquad (3)$$

Equation 3 represents concisely a system of nine simultaneous linear equations that determine the spatial orientation of the tomographic section relative to the stereotactic frame. This equation transforms the (u_1, v_1), (u_2, v_2), and (u_3, v_3) coordinates from the two-dimensional coordinate system of the tomographic image to create (x_1, y_1, z_1), (x_2, y_2, z_2), and (x_3, y_3, z_3) coordinates in the three-dimensional coordinate system of the stereotactic frame.

In Equation 3, the matrix elements x_1, y_1, z_1, x_2, y_2, z_2, x_3, y_3, and z_3, as well as the matrix elements u_1, v_1, u_2, v_2, u_3, and v_3, are known. The matrix elements m_{11} through m_{33} are unknown; hence, Equation 3 may be inverted to solve for these unknown elements of the transformation matrix

$$\begin{bmatrix} m_{11} & m_{12} & m_{13} \\ m_{21} & m_{22} & m_{23} \\ m_{31} & m_{32} & m_{33} \end{bmatrix} = \begin{bmatrix} u_1 & v_1 & 1 \\ u_2 & v_2 & 1 \\ u_3 & v_3 & 1 \end{bmatrix}^{-1} \begin{bmatrix} x_1 & y_1 & z_1 \\ x_2 & y_2 & z_2 \\ x_3 & y_3 & z_3 \end{bmatrix} \qquad (4)$$

where the exponent "-1" indicates the inverse of the matrix that contains the elements u_1, v_1, u_2, v_2, u_3, and v_3. The inverse of this matrix exists and may be calculated to high precision if this matrix is non-singular, that is, if the three points (u_1, v_1), (u_2, v_2), and (u_3, v_3) are not collinear [4].

Once the transformation matrix elements m_{11} through m_{33} are known, the (u_T, v_T) coordinates of the target point P_T may be transformed from the two-dimensional coordinate system of the tomographic image into the three-dimensional coordinate system of the stereotactic frame to obtain the (x_T, y_T, z_T) coordinates of the analogous target point P'_T

$$\begin{bmatrix} x_T & y_T & z_T \end{bmatrix} = \begin{bmatrix} u_T & v_T & 1 \end{bmatrix} \begin{bmatrix} m_{11} & m_{12} & m_{13} \\ m_{21} & m_{22} & m_{23} \\ m_{31} & m_{32} & m_{33} \end{bmatrix} \qquad (5)$$

Equation 5 has been used for the past 36 years to calculate the (x_T, y_T, z_T) coordinates of the target point P'_T in the three-dimensional coordinate system of the stereotactic frame [7-8]. Despite its ubiquitous use, this equation applies to only three N-localizers. Some applications of the N-localizer have incorporated four N-localizers [9-14] and hence have required that one of the four N-localizers be ignored in order to apply Equation 5. Recently, however, the mathematics of the N-localizer have been extended to apply to three or more N-localizers and thus have eliminated the requirement to discard one of the N-localizers [5]. A further extension of the mathematics of the N-localizer enables the application of the N-localizer to volume imaging, as discussed in the remainder of this article.

Materials And Methods

Magnetic resonance (MR) imaging differs from computed tomography (CT) imaging in the manner by which the images are obtained. CT obtains a volume of individual tomographic images of the patient by changing the position of the scanner bed between successive tomographic scans and hence is susceptible to errors in scanner bed positioning. MR obtains a volume image of the patient by applying magnetic field gradients [15] and thus does not require changing the position of the scanner bed. Indeed, MR may obtain a volume image of the patient directly without obtaining a series of planar, tomographic scans. Because MR is not susceptible to errors in scanner bed positioning, the spatial accuracy of a MR volume image ought to be greater than the spatial accuracy of a volume of successive CT images, provided that the patient does not move during the imaging procedure.

A volume image comprises individual volume elements, or voxels, that are identified via their (u, v, w) coordinates in the same manner that the individual picture elements, or pixels, from a planar, tomographic image are identified via their (u, v) coordinates. A planar section of these voxels is a subset of the voxels wherein one of the (u, v, w) coordinates is held constant. An axial plane has constant w and varying (u, v) coordinates. A sagittal plane has constant u and varying (v, w) coordinates. A coronal plane has constant v and varying (u, w) coordinates. In this context, the term "planar section" or "plane" designates an axial, sagittal, or coronal plane, i.e., a subset of the voxels that one volume image comprises. Such a plane is to be distinguished from a tomographic image that comprises a set of pixels that are obtained via one planar, tomographic scan.

A MR localizer frame differs from a CT localizer frame in that the MR localizer frame is designed to create fiducials in sagittal and coronal planes in addition to axial planes [16]. A MR localizer frame comprises five N-localizers that subtend the anterior, posterior, left, right, and superior faces of a cube that encloses the patient's head (Figure *5*).
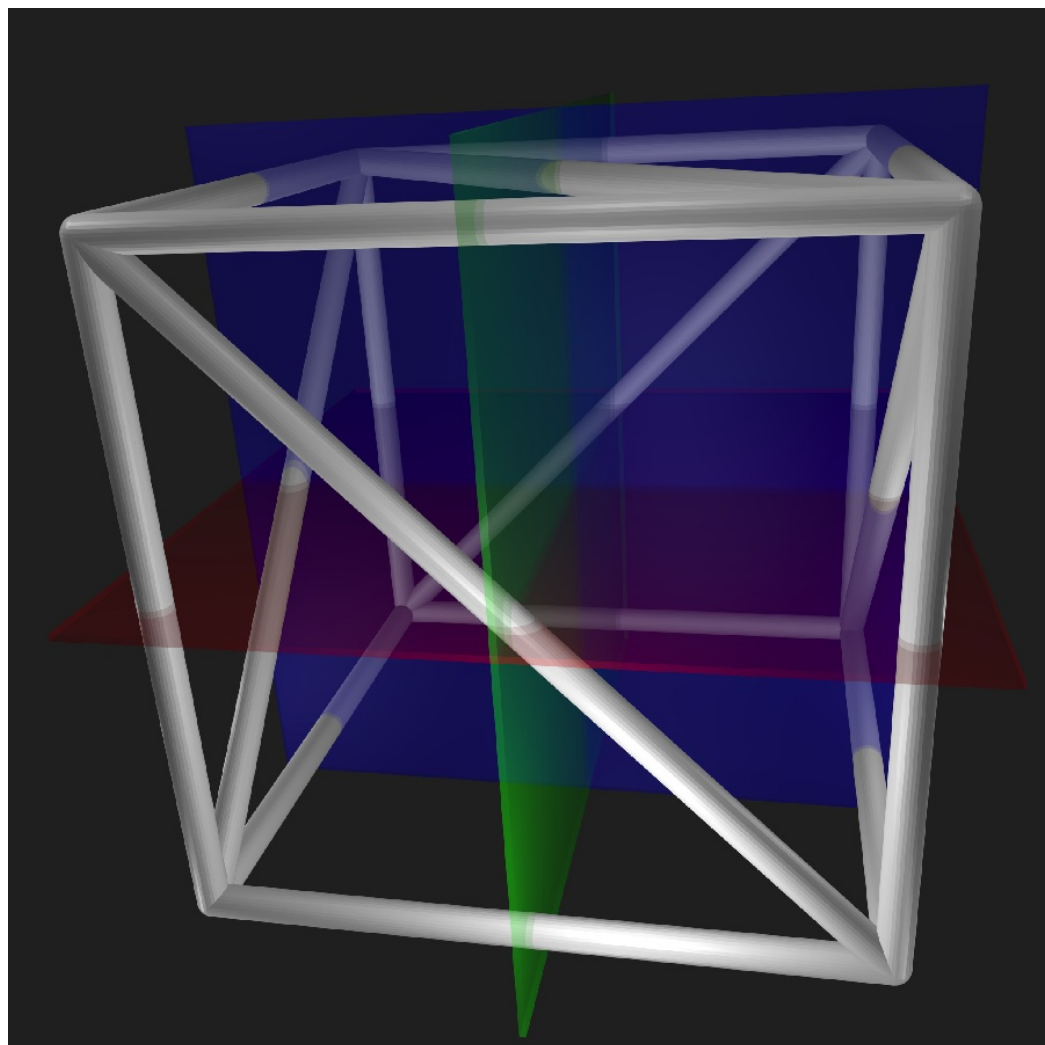
FIGURE 5: MR localizer frame and axial, sagittal and coronal planes

A MR localizer frame comprises five N-localizers that subtend the anterior, posterior, left, right and superior faces of a cube. An axial plane (red) intersects the MR localizer frame at four N-localizers: anterior, posterior, left and right. A sagittal plane (green) intersects the MR localizer frame at three N-localizers: anterior, posterior and superior. A coronal plane (blue) intersects the MR localizer frame at three N-localizers: left, right and superior.

In a manner analogous to Equation 3, the spatial orientation of MR voxel data may be determined relative to the stereotactic frame. The equation that applies to these voxel data requires four (x, y, z) coordinates (x_1, y_1, z_1), (x_2, y_2, z_2), (x_3, y_3, z_3), and (x_4, y_4, z_4) from the three-dimensional coordinate system of the stereotactic frame. This equation also requires four (u, v, w) coordinates (u_1, v_1, w_1), (u_2, v_2, w_2), (u_3, v_3, w_3), and (u_4, v_4, w_4) from the three-dimensional coordinate system of the voxel data. The (u, v, w) coordinates are the centers of ellipses B_i that are visualized in axial, sagittal, or coronal planes of the voxel data, similar to the approach that is discussed for an axial tomographic section in Figure 4. The (x, y, z) coordinates are calculated from the (u, v, w) coordinates of the centers of circles A_i and C_i and ellipses B_i via Equation 1 or Equation 2.

The spatial orientation of the voxel data relative to the stereotactic frame is specified using the

matrix equation [17]

$$\begin{bmatrix} x_1 & y_1 & z_1 & 1 \\ x_2 & y_2 & z_2 & 1 \\ x_3 & y_3 & z_3 & 1 \\ x_4 & y_4 & z_4 & 1 \end{bmatrix} = \begin{bmatrix} u_1 & v_1 & w_1 & 1 \\ u_2 & v_2 & w_2 & 1 \\ u_3 & v_3 & w_3 & 1 \\ u_4 & v_4 & w_4 & 1 \end{bmatrix} \begin{bmatrix} m_{11} & m_{12} & m_{13} & 0 \\ m_{21} & m_{22} & m_{23} & 0 \\ m_{31} & m_{32} & m_{33} & 0 \\ m_{41} & m_{42} & m_{43} & 1 \end{bmatrix} \qquad (6)$$

Equation 6 represents concisely a system of 12 simultaneous linear equations that determine the spatial orientation of the voxel data relative to the stereotactic frame. This equation transforms the (u_1, v_1, w_1) , (u_2, v_2, w_2) , (u_3, v_3, w_3) , and (u_4, v_4, w_4) coordinates from the three-dimensional coordinate system of the voxel data to create (x_1, y_1, z_1) , (x_2, y_2, z_2) , (x_3, y_3, z_3) , and (x_4, y_4, z_4) coordinates in the three-dimensional coordinate system of the stereotactic frame.

One important restriction applies to Equation 6. The four (u, v, w) coordinates (u_1, v_1, w_1) , (u_2, v_2, w_2) , (u_3, v_3, w_3) , and (u_4, v_4, w_4) must not be coplanar; hence, these four (u, v, w) coordinates must not be obtained from a single plane, such as an axial plane that comprises four fiducials. Thus, one of many acceptable sets of (u, v, w) coordinates would comprise two (u, v, w) coordinates from the left and right N-localizers that intersect an axial plane, plus two (u, v, w) coordinates from the anterior and superior N-localizers that intersect a sagittal plane. This restriction is similar to the restriction that applies to Equation 3, i.e., three noncollinear (u, v) coordinates must be used in Equation 3 [4].

In Equation 6, the matrix elements x_1 , y_1 , z_1 , x_2 , y_2 , z_2 , x_3 , y_3 , z_3 , x_4 , y_4 , and z_4 , as well as the matrix elements u_1 , v_1 , w_1 , u_2 , v_2 , w_2 , u_3 , v_3 , w_3 , u_4 , v_4 , and w_4 , are known. The matrix elements, m_{11} through m_{43} , are unknown; hence, it is possible (and tempting) to invert Equation 6 in order to solve for these unknown elements of the transformation matrix in a similar manner to the inversion of Equation 3 that yields Equation 4. However, a more useful solution may be obtained by applying the method of least squares to more than four sets of fiducials because the method of least squares minimizes the effect of errors in the voxel data [18].

For voxel data, a useful set of fiducials would comprise ten fiducials: four fiducials from an axial plane, three fiducials from a sagittal plane, and three fiducials from a coronal plane, where the target point P_T is visualized in all three planes. The following equation transforms ten (u, v, w) coordinates from the three-dimensional coordinate system of the voxel data to create ten (x, y, z) coordinates in the three-dimensional coordinate system of the stereotactic frame

$$\begin{bmatrix} x_i & y_i & z_i & 1 \end{bmatrix} = \begin{bmatrix} u_i & v_i & w_i & 1 \end{bmatrix} \begin{bmatrix} m_{11} & m_{12} & m_{13} & 0 \\ m_{21} & m_{22} & m_{23} & 0 \\ m_{31} & m_{32} & m_{33} & 0 \\ m_{41} & m_{42} & m_{43} & 1 \end{bmatrix} \qquad (7)$$

where the subscript i selects one of the ten fiducials. The equations that are required for least-squares minimization are obtained by first expanding the matrix multiplication of Equation 7 and expressing the result for the matrix elements x_i , y_i and z_i

$$x_i = u_i m_{11} + v_i m_{21} + w_i m_{31} + m_{41}$$
$$y_i = u_i m_{12} + v_i m_{22} + w_i m_{32} + m_{42} \qquad (8)$$
$$z_i = u_i m_{13} + v_i m_{23} + w_i m_{33} + m_{43}$$

In the presence of error, Equation 8 may be modified to express the errors in x_i, y_i, and z_i, respectively, as δx_i, δy_i, and δz_i

$$\delta x_i = x_i - u_i m_{11} - v_i m_{21} - w_i m_{31} - m_{41}$$
$$\delta y_i = y_i - u_i m_{12} - v_i m_{22} - w_i m_{32} - m_{42} \qquad (9)$$
$$\delta z_i = z_i - u_i m_{13} - v_i m_{23} - w_i m_{33} - m_{43}$$

In order to minimize these errors via the method of least squares, the equations for δx_i, δy_i, and δz_i are squared to obtain the error functions E_x, E_y, and E_z

$$E_x\left(m_{11}, m_{21}, m_{31}, m_{41}\right) = \sum \left(x_i - u_i m_{11} - v_i m_{21} - w_i m_{31} - m_{41}\right)^2$$
$$E_y\left(m_{12}, m_{22}, m_{32}, m_{42}\right) = \sum \left(y_i - u_i m_{12} - v_i m_{22} - w_i m_{32} - m_{42}\right)^2 \qquad (10)$$
$$E_z\left(m_{13}, m_{23}, m_{33}, m_{43}\right) = \sum \left(z_i - u_i m_{13} - v_i m_{23} - w_i m_{33} - m_{43}\right)^2$$

The following discussion illustrates minimization of the error function E_x; minimization of the error functions E_y and E_z is performed in an analogous manner. At the minimum of a function, all of the derivatives are equal to zero. Evaluating the derivatives $\partial E_x / \partial m_{11}$, $\partial E_x / \partial m_{21}$, $\partial E_x / \partial m_{31}$, and $\partial E_x / \partial m_{41}$ and setting the resulting expressions for these derivatives to zero yields

$$\partial E_x / \partial m_{11} = \sum 2\left(x_i - u_i m_{11} - v_i m_{21} - w_i m_{31} - m_{41}\right) u_i = 0$$
$$\partial E_x / \partial m_{21} = \sum 2\left(x_i - u_i m_{11} - v_i m_{21} - w_i m_{31} - m_{41}\right) v_i = 0$$
$$\partial E_x / \partial m_{31} = \sum 2\left(x_i - u_i m_{11} - v_i m_{21} - w_i m_{31} - m_{41}\right) w_i = 0 \qquad (11)$$
$$\partial E_x / \partial m_{41} = \sum 2\left(x_i - u_i m_{11} - v_i m_{21} - w_i m_{31} - m_{41}\right) = 0$$

Simplifying and rearranging the above equations for the derivatives yields a system of four simultaneous linear equations of the four unknowns m_{11}, m_{21}, m_{31}, and m_{41}

$$m_{11} \sum u_i^2 + m_{21} \sum u_i v_i + m_{31} \sum u_i w_i + m_{41} \sum u_i = \sum u_i x_i$$
$$m_{11} \sum u_i v_i + m_{21} \sum v_i^2 + m_{31} \sum v_i w_i + m_{41} \sum v_i = \sum v_i x_i$$
$$m_{11} \sum u_i w_i + m_{21} \sum v_i w_i + m_{31} \sum w_i^2 + m_{41} \sum w_i = \sum w_i x_i \qquad (12)$$
$$m_{11} \sum u_i + m_{21} \sum v_i + m_{31} \sum w_i + m_{41} n = \sum x_i$$

where n is the number of sets of fiducials; in this case, $n = 10$. These simultaneous linear equations may be solved using Cramer's rule [19] to yield the matrix elements m_{11}, m_{21}, m_{31}, and m_{41} that minimize the error function E_x as follows. Each of the elements m_{11}, m_{21}, m_{31}, and m_{41} that are found in the first column of the transformation matrix and that minimize E_x may be calculated as the ratio of two determinants wherein the denominator determinant contains the sums from Equation 12

$$\begin{vmatrix} \sum u_i^2 & \sum u_i v_i & \sum u_i w_i & \sum u_i \\ \sum u_i v_i & \sum v_i^2 & \sum v_i w_i & \sum v_i \\ \sum u_i w_i & \sum v_i w_i & \sum w_i^2 & \sum w_i \\ \sum u_i & \sum v_i & \sum w_i & n \end{vmatrix} \qquad (13)$$

and wherein the numerator determinant for the calculation of m_{11}, m_{21}, m_{31}, and m_{41},

respectively, is obtained by replacing the first, second, third, and fourth columns of Equation 13 with

$$\begin{bmatrix} \sum u_i x_i \\ \sum v_i x_i \\ \sum w_i x_i \\ \sum x_i \end{bmatrix} \qquad (14)$$

Similarly, each of the elements m_{12}, m_{22}, m_{32}, and m_{42} that are found in the second column of the transformation matrix and that minimize E_y may be calculated as the ratio of two determinants wherein the denominator determinant is shown in Equation 13 and wherein the numerator determinant for the calculation of m_{12}, m_{22}, m_{32}, and m_{42}, respectively, is obtained by replacing the first, second, third, and fourth columns of Equation 13 with

$$\begin{bmatrix} \sum u_i y_i \\ \sum v_i y_i \\ \sum w_i y_i \\ \sum y_i \end{bmatrix} \qquad (15)$$

Finally, each of the elements m_{13}, m_{23}, m_{33}, and m_{43} that are found in the third column of the transformation matrix and that minimize E_z may be calculated as the ratio of two determinants wherein the denominator determinant is shown in Equation 13 and wherein the numerator determinant for the calculation of m_{13}, m_{23}, m_{33}, and m_{43}, respectively, is obtained by replacing the first, second, third, and fourth columns of Equation 13 with

$$\begin{bmatrix} \sum u_i z_i \\ \sum v_i z_i \\ \sum w_i z_i \\ \sum z_i \end{bmatrix} \qquad (16)$$

In this manner, the 12 elements of the transformation matrix may be obtained, such that these matrix elements minimize the error functions, E_x, E_y, and E_z.

Once the elements, m_{11} through m_{43}, of the transformation matrix have been calculated as discussed above, the transformation matrix may be used as follows to transform the (u_T, v_T, w_T) coordinates of the target point P_T from the three-dimensional coordinate system of the voxel data into the three-dimensional coordinate system of the stereotactic frame to obtain the (x_T, y_T, z_T) coordinates of the analogous target point P_T'

$$\begin{bmatrix} x_T & y_T & z_T & 1 \end{bmatrix} = \begin{bmatrix} u_T & v_T & w_T & 1 \end{bmatrix} \begin{bmatrix} m_{11} & m_{12} & m_{13} & 0 \\ m_{21} & m_{22} & m_{23} & 0 \\ m_{31} & m_{32} & m_{33} & 0 \\ m_{41} & m_{42} & m_{43} & 1 \end{bmatrix} \qquad (17)$$

The accuracy of the calculation of elements m_{11} through m_{43} of the transformation matrix, and hence the accuracy of the transformation of the (u_T, v_T, w_T) coordinates, is indicated by the three correlation coefficients, r_x, r_y and r_z, that express how well the right-hand sides of Equation 8 estimate the left-hand sides of that equation [20]. Taking the first of Equations 8 as an example, the correlation coefficient r_x that measures the correlation between the right-

hand side

$$\epsilon_i = m_{11}u_i + m_{21}v_i + m_{31}w_i + m_{41} \qquad (18)$$

and the left-hand side x_i is calculated as [21]

$$r_x = \frac{n \sum \epsilon_i x_i - \sum \epsilon_i \sum x_i}{\sqrt{n \sum \epsilon_i^2 - \left(\sum \epsilon_i\right)^2}\sqrt{n \sum x_i^2 - \left(\sum x_i\right)^2}} \qquad (19)$$

The correlation coefficients r_y and r_z are calculated in an analogous manner.

Results

The author has access to neither a MR localizer frame nor a MR scanner, so this article discusses mathematics rather than experimental results. The reader is encouraged to read the Results and Discussion sections of "The Mathematics of Three or More N-Localizers for Stereotactic Neurosurgery" [5] that discuss the correlation coefficient r_{xyz} that is calculated for a single tomographic image. The correlation coefficients, r_x, r_y, and r_z, that are calculated for a volume image permit a similar analysis of image data.

Discussion

Equations 7-17 provide a method for transforming (u, v, w) coordinates from the three-dimensional coordinate system of voxel data, which are obtained via volume imaging, into the three-dimensional coordinate system of the stereotactic frame to produce (x, y, z) coordinates. These equations require the use of four or more pairs of noncoplanar (u, v, w) and (x, y, z) coordinates. A useful set of (u, v, w) and (x, y, z) coordinates may be obtained from axial, sagittal, and coronal planes, in which the target point P_T is visualized, by selecting the (u, v, w) coordinates then calculating the (x, y, z) coordinates via Equation 1 or 2. Although the axial, sagittal, and coronal planes in which the target point is visualized would appear to be the most useful of the image planes, there is no requirement to include these particular planes in the calculation of elements, m_{11} through m_{43}, of the transformation matrix via Equations 7-16. Because the transformation matrix transforms (u, v, w) coordinates from the three-dimensional coordinate system of the voxel data to produce (x, y, z) coordinates in the three-dimensional coordinate system of the stereotactic frame, all of the (u, v, w) coordinates from the voxel data are transformed into (x, y, z) coordinates, independent of the specific planes from which the (u, v, w) coordinates are selected for application of Equations 1-2 and 7-17.

An alternative to Cramer's rule is Gauss elimination [22] that is more computationally efficient than Cramer's rule and that, in principle, results in less numerical error. However, in practice, Cramer's rule is sufficient for the purposes of this article so long as at least four noncoplanar points are used in Equation 7.

Equations 7-16 and 18-19 permit the calculation of the correlation coefficients r_x, r_y, and r_z that provide a measure of the accuracy of the transformation. The accuracy of the transformation is degraded by nonlinear distortion to which MR data are susceptible. This nonlinear distortion may be caused by metallic elements of the stereotactic frame, inhomogeneity and temporal fluctuation of the magnetic field, and metallic equipment near the MR scanner [23-27].

In view of this susceptibility to nonlinear distortion, an assessment of the nonlinear distortion may be improved through the use of additional (u, v, w) and (x, y, z) coordinates that may be obtained from axial, sagittal, and coronal planes that do not include the target point P_T. These additional planes could be chosen from throughout the volume image; their (u, v, w) and (x, y, z) coordinates would contribute to the calculation of the correlation coefficients r_x, r_y, and r_z and thereby provide a measure of the presence of nonlinear distortion within the volume image.

MR scanners are equipped with small "shimming" electromagnets that are used to increase the homogeneity of the magnetic field and hence improve the linearity of MR images. Because the optimum shim settings differ between patients, these optimum shim settings should be determined for each patient individually. A MR localizer frame could assist in the determination of the optimum shim settings as follows. A volume image that comprises voxel data could be obtained for a patient wearing a MR localizer frame, then (u, v, w) coordinates could be chosen from throughout that volume image. The (x, y, z) coordinates could be calculated via Equation 1 or 2, then the elements m_{11} through m_{43} of the transformation matrix and the correlation coefficients r_x, r_y, and r_z could be calculated from the (u, v, w) and (x, y, z) coordinates via Equations 7-16 and 18-19. These correlation coefficients would provide an analysis of the linearity of the voxel data and hence provide an indication of the quality of the shimming procedure.

Conclusions

This article describes mathematics that permit the transformation of (u, v, w) coordinates from the three-dimensional coordinate system of voxel data, which are obtained via MR scanning, into the three-dimensional coordinate system of the stereotactic frame to produce (x, y, z) coordinates. The mathematics also permit the calculation of correlation coefficients that provide a statistical measure of the presence of nonlinear distortion in the voxel data.

Additional Information

Disclosures

Conflicts of interest: The authors have declared that no conflicts of interest exist.

Acknowledgements

References

1. Brown RA, Nelson JA: Invention of the N-localizer for stereotactic neurosurgery and its use in the Brown-Roberts-Wells stereotactic frame. Neurosurg. 2012, 70:173-6. 10.1227/NEU.0b013e318246a4f7
2. Brown RA, Nelson JA: The origin of the N-localizer for stereotactic neurosurgery . http://www.cureus.com. 2013, 5:E140. Accessed: November 21, 2014: http://www.cureus.com/articles/2335-the-origin-of-the-n-localizer-for-stereotactic-neurosurgery.
3. Brown RA: The mathematics of the N-localizer for stereotactic neurosurgery . http://www.cureus.com. 2013, 5:e142. Accessed: November 21, 2014: http://www.cureus.com/articles/2335-the-origin-of-the-n-localizer-for-stereotactic-neurosurgery.
4. Brown RA, Nelson JA: The history and mathematics of the N-localizer for stereotactic neurosurgery. http://www.cureus.com. 2014, 6:e156. Accessed: November 21, 2014:

http://www.cureus.com/articles/2391-the-history-and-mathematics-of-the-n-localizer-for-stereotactic-neurosurgery.

5. Brown RA: The mathematics of three or more N-localizers for stereotactic neurosurgery . http://www.cureus.com. 2014, 6:e218. Accessed: November 21, 2014: http://www.cureus.com/articles/2645-the-mathematics-of-three-or-more-n-localizers-for-stereotactic-neurosurgery .

6. Brown RA: A computerized tomography-computer graphics approach to stereotaxic localization. J Neurosurg. 1979, 50:715-20. 10.3171/jns.1979.50.6.0715

7. Brown RA: A stereotactic head frame for use with CT body scanners . Invest Radiol. 1979, 14:300-4. 10.1097/00004424-197907000-00006

8. Brown RA, Roberts TS, Osborn AG: Stereotaxic frame and computer software for CT-directed neurosurgical localization. Invest Radiol. 1980, 15:308-12. 10.1097/00004424-198007000-00006

9. Perry JH, Rosenbaum AE, Lunsford LD, Swink CA, Zorub DS: Computed tomography/guided stereotactic surgery: conception and development of a new stereotactic methodology. Neurosurg. 1980, 7:376-81. 10.1227/00006123-198010000-00011

10. Dubois PJ, Nashold BS, Perry J, Burger P, Bowyer K, Heinz ER, Drayer BP, Bigner S, Higgins AC: CT-guided stereotaxis using a modified conventional stereotaxic frame . AJNR Am J Neuroradiol. 1982, 3:345-51.

11. Thomas DG, Anderson RE, du Boulay GH: CT-guided stereotactic neurosurgery: Experience in 24 cases with a new stereotactic system. J Neurol Neurosurg Psychiatry. 1984, 47:9-16. 10.1136/jnnp.47.1.9

12. Bullard DE, Nashold BS Jr, Osborne D, Burger PC, Dubois P: CT-guided stereotactic biopsies using a modified frame and Gildenberg techniques. J Neurol Neurosurg Psychiatry. 1984, 47:590-5. 10.1136/jnnp.47.6.590

13. Maciunas RJ, Kessler RM, Maurer C, Mandava V, Watt G, Smith G: Positron emission tomography imaging-directed stereotactic neurosurgery. Stereotact Funct Neurosurg. 1992, 58:134-40. 10.1159/000098986

14. Levivier M, Massager N, Wikler D, Lorenzoni J, Ruiz S, Devriendt D, David P, Desmedt F, Simon S, Van Houtte P, Brotchi J, Goldman S: Use of stereotactic PET images in dosimetry planning of radiosurgery for brain tumors: clinical experience and proposed classification. J Nucl Med. 2004, 45:1146-54.

15. Callaghan PT: Principles of Nuclear Magnetic Resonance Microscopy . Oxford University Press, Oxford [England], New York; pp. 121-132, 1991.

16. Cosman ER: Means for localizing target coordinates in a body relative to a guidance system reference frame in any arbitrary plane as viewed by a tomographic image through the body. United States Patent 4618978. 1986, pp 1-7. Accessed: November 21, 2014: http://www.freepatentsonline.com/4618978.html.

17. Newman WM, Sproull RF: Principles of interactive computer graphics . McGraw-Hill Book Company, New York; 1979, pp 333-336.

18. Kreyszig E, Kreyszig H, Norminton EJ: Advanced engineering mathematics (10th ed). John Wiley and Sons, Inc, Hoboken, New Jersey; 2011, pp 872-875.

19. Kreyszig E, Kreyszig H, Norminton EJ: Advanced engineering mathematics (10th ed). John Wiley and Sons, Inc, Hoboken, New Jersey; 2011, pp 298-299.

20. Spiegel MR: Schaum's outline series. Theory and problems of statistics . McGraw-Hill Book Company, New York; 1961, pp 243-244.

21. Spiegel MR: Schaum's outline series. Theory and problems of statistics . McGraw-Hill Book Company, New York; 1961, pp 271.

22. Kreyszig E, Kreyszig H, Norminton EJ: Advanced engineering mathematics. (10th ed). John Wiley and Sons, Inc, Hoboken, New Jersey; 2011, pp 272-280.

23. Leksell L, Leksell D, Schwebel J: Stereotaxis and nuclear magnetic resonance . J Neurol Neurosurg Psychiatry. 1985, 48:14-8. 10.1136/jnnp.48.1.14

24. Thomas DG, Davis CH, Ingram S, Olney JS, Bydder GM, Young IR: Stereotaxic biopsy of the brain under MR imaging control. AJNR Am J Neuroradiol. 1986, 7:161-3.

25. Heilbrun MP, Sunderland PM, McDonald PR, Wells TH Jr, Cosman E, Ganz E: Brown-Roberts-Wells stereotactic frame modifications to accomplish magnetic resonance imaging guidance in three planes. Appl Neurophysiol. 1987, 50:143-52.

26. Andoh K, Nakamae H, Ohkoshi T, Odagiri K, Kyuma Y, Hayashi: Technical note: Enhanced

MR-guided stereotaxic brain surgery with the patient under general anesthesia. AJNR Am J Neuroradiol. 1991, 12:135-138.

27. Kondziolka D, Dempsey PK, Lunsford LD, Kestle JR, Dolan EJ, Kanal E, Tasker RR: A comparison between magnetic resonance imaging and computed tomography for stereotactic coordinate determination. Neurosurg. 1992, 30:402-6. 00006123-199203000-00015